J. Hydrol. Hydromech., 64, 2016, 2, 167–175
DOI: 10.1515/johh-2016-0010

Spatial patterns of wetting characteristics in grassland sandy soil

Tomáš Orfánus[1*], Dagmar Stojkovová[1], Kálmán Rajkai[2], Henryk Czachor[3], Renáta Sándor[2]

[1] Institute of Hydrology, Slovak Academy of Sciences, Dúbravská 9, 841 04 Bratislava, Slovak Republic.
[2] Research Institute for Soil Science and Agricultural Chemistry of the Hungarian Academy of Sciences, Herman Otto ut. 24, 1022 Budapest, Hungary.
[3] Polish Academy of Sciences Institute of Agrophysics, ul. Doswiadczalna 4, P.O. Box 201, 20-290 Lublin, Poland.
[*] Corresponding author. E-mail: orfanus@uh.savba.sk

Abstract: In grasslands where organic and inorganic resources are alternating at scales of individual plants, the transient character is given to certain wetting properties of soil, which then become highly variable both in space and in time. The objective of presented study was to study wetting pattern within two soil horizons at 5-cm and 10-cm depths respectively and to examine how the wetting patterns relate to hydraulic conductivity determined by Minidisc infiltrometer at suction –2 cm, $K_{(-2\ \mathrm{cm})}$. This characteristics is implicitly independent on antecedent soil water content (SWC) since it relates to steady infiltration phase but can be influenced by present soil water repellency (SWR). Field measurements were performed on July 27–28, 2010 on the grassland experimental site located near the village Sekule in Southwest Slovakia. The water drop penetration time (WDPT), SWC and tension Minidisc infiltration measurements were carried out on the 0.64 m^2 plot in a regular 8 x 8 grid. The results showed that SWR and SWC influence each other and cause correlation between spatial patterns of studied soil wetting characteristics and between characteristics measured at the two soil depths. Further, it was found out, that calculation of $K_{(-2\ \mathrm{cm})}$ according to Zhang may cause apparent correlation of $K_{(-2\ \mathrm{cm})}$ with antecedent SWC, which is the artificial effect of sorptivity parameter in the equation on steady stage of infiltration process. This pseudocorrelation has disappeared after adopting of Minasny and McBratney (2000) approaches by calculation of $K_{(-2\ \mathrm{cm})}$.

Keywords: Soil wetting pattern; Soil water repellency; Hydraulic conductivity; Sorptivity; Arenosol.

INTRODUCTION

Assessment of soil hydraulic properties is very important component for the interpretation of the physical characteristics of soil and the management of agricultural practices (Green et al., 2003). The information about their spatial and temporal variability and patterns is useful also for many other applications (forest and grassland management, erosion control, waste and contaminants management etc.). The knowledge about this issue has become quite robust during the last half century in rigid and relatively uniform soils but certain part of this knowledge should be handled carefully when dealing with heavy soils, stony soils, soils with high organic matter content or water repellent soils (Bedrna and Orfánus, 2013). Infiltration is critical process for example in grasslands, where the resources such as water, litter, nutrients and biological activity are typically scaled at the level of individual plants (Schlesinger et al., 1996) and where their synergism may frequently result in water repellency of soil and uneven wetting pattern. Soil water repellency (SWR) reduces the affinity of soils to water in a way that they resist wetting for periods ranging from a few seconds to hours, days or weeks (Doerr and Thomas, 2000). It has hydrological and geomorphological repercussions for example such as the reduced infiltration capacity of soils, enhanced overland flow and accelerated soil erosion, development of preferential flow and the accelerated leaching of agrochemicals (e.g. Ritsema el al., 1997). The persistence (Dekker et al., 1999) or stability (Letey et al., 2000) of SWR can be estimated by the water drop penetration time (WDPT) test (Dekker and Ritsema, 1994). The severity of SWR can be estimated by the ninety degree surface tension, contact angle or the molarity of an ethanol droplet (MED) test (Kořenková et al., 2015; Letey et al., 2000). The repellency index R_I is a measure of intrinsic sorptivity of soil and calculated from the ratio of soil sorptivities for ethanol and water (Tillman et al., 1989). Using the algorithm resembling Monte Carlo method, the repellency index was spatially interpreted by Pekárová et al. (2015).

Particularly coarse-textured soils will be susceptible to soil water repellency development after prolonged dry periods and elevated temperatures (Mataix-Solera et al., 2008) that could occur more often from climate change (Goebel et al., 2011). It is because of their low specific surface, which can easily be covered by hydrophobic substances. The majority of works assessing soil wettability were carried out in arid or semiarid regions (e.g. Leighton-Boyce et al., 2005). The studies dealing with the occurence of SWR in temperate or more humid climatic regions were, thus, carried out mainly on coarse textured (sandy) soils (Täumer et al., 2005) or those situated in coastal areas at low altitude (Dekker et al., 2001).

Many studies on hydraulics of water repellent soils have been performed during the last decades (e.g. Dekker et al., 1999; Doerr et al., 2000; Hallett et al., 2004; Lichner et al., 2003, 2011; Orfánus et al., 2014; Ritsema et al., 1997, 2005). Soil hydraulic conductivity is the most important hydrodynamic characteristics in most water-related studies in soil and on many physical processes active on its surface. It is a function of water potential or water content of the soil. It is steeply decreasing as the soil dries primarily due to the movement of air into the soil to replace the water. The pathways for water flow between soil particles become smaller and more tortuous, and flow becomes more difficult (Taiz et al., 2015).

Disk infiltrometers are established as standard devices for measuring soil surface hydraulic properties when large macropores and cracks should be avoided from the infiltration process (Dohnal et al., 2010). By application of small suction (typically 0–10 cm) at the soil-disc interface the unsaturated (in wettable soils also called the near-saturated) hydraulic conductivity is being usually obtained from the disk infiltrometer data.

Fodor et al. (2011) dealt with three field types of saturated hydraulic conductivity measuring methods, which were investigated and compared using *in situ* infiltration data, as well as outflow data obtained from two laboratory methods. They found substantial variability of hydraulic conductivity determined by different measurement and calculation methods. Measuring soil hydraulic conductivity with a minidisk infiltrometer was proposed by Zhang (1997), where the method requires measuring of cumulative infiltration vs. time and fitting the results to compute sorptivity and the hydraulic conductivity of soil.

Minasny and McBratney (2000) analyzed infiltration data from the numerical experiment and the field study as well to obtain the estimate of sorptivity by five fitting methods (different from Zhang's) and incorporation of such estimated sorptivity for calculation of $K_{(-2\ \mathrm{cm})}$ based on Wooding (1968) and White and Sully (1987). This approach eliminated the effect of initial unsaturation of soil on $K_{(-2\ \mathrm{cm})}$ values, which was not treated in the method of Zhang (1997).

The unsaturated hydraulic conductivity measured using Mini Disk Infiltrometer and calculated according Zhang (1997) and Wooding (1968) was also discussed in Kodešová et al. (2011). Authors report overestimation of values provided by Zhang's method. Orfánus et al. (2014) observed statistically significant temporal changes in $K_{(-2\ \mathrm{cm})}$ calculated according to Zhang (1997) in severally water repellent soil near Sekule in Slovakia. Authors explained this unexpected behavior by temporal changes in distribution of water repellent vs. wettable soil domains (wetting pattern).

Close et al. (1998) observed a non-uniform wetting pattern of the sand at the membrane interface. This has resulted in differences in infiltration rate and variations in infiltrating area and depth of infiltration. The maximum difference in infiltration was 80% and the infiltration area varied from 25% to 100%. The non-uniform wetting of soil led to a high variation in infiltration curves also in Minasny and McBratney (2000).

The objective of here presented research was to analyze the spatial variability of unsaturated hydraulic conductivity, $K_{(-2\ \mathrm{cm})}$ within two horizons of water repellent sandy soil under the grassland vegetation with respect to overall wetting pattern and observed water repellency within these horizons. Two different fitting methods for $K_{(-2\ \mathrm{cm})}$ calculation from minidisk infiltration tests proposed by Zhang (1997) and Minasny and McBratney (2000) were applied to provide deeper insight into the observed relationships.

MATERIALS AND METHODS
Locality Mlaky II

The experimental site Mlaky II near Sekule in Southwestern Slovakia is located at an elevation of 150 m above sea level with the average annual air temperature of 9.8°C, and the annual precipitation of 500–600 mm. The soil is classified as *Acid Aeolic Arenosol* (WRB, 2014), evolved from combined fluvial and aeluvial sandy sediments giving it a sandy texture (91.3% of sand, 2.8% of silt and 5.9% of clay). The soil contains organic carbon (0.99%) and its soil reaction is acidic (pH-H_2O = 5.14). The former pine-forest (*Pinus sylvestris*) had been removed and the actual vegetation consists mostly of grass species (*Poaceae* family). Among other species most frequent are *Achillea millefolium, Acetosella vulgaris, Anthemis ruthenica*, *Convolvulus arvensis, Lepidium ruderale, Plantago lanceolata* and *Potentilla sp*. The moss *Brachythecium albicans* appears amply, too.

Data collecting

Field measurements were performed on the 1 m^2 plot situated on the grassland area at Mlaky II location in July 27–28, 2010. The site for the research plot was visually selected with respect to maximize variability of vegetation species. The vegetation had been removed with its uppermost root zone to the depths of 5 cm. The water drop penetration time (WDPT), soil water contents (SWC) and tension minidisc infiltration measurements were carried out on treated inner 80 x 80 cm of the 1x1m plot according to the scheme in Fig. 1, which provided

	1	2	3	4	5	6	7	8
1	$K_{(-2\ \mathrm{cm})}$ S WDPT	θ WDPT	$K_{(-2\ \mathrm{cm})}$ S WDPT	θ WDPT	$K_{(-2\ \mathrm{cm})}$ S WDPT	θ WDPT	$K_{(-2\ \mathrm{cm})}$ S WDPT	θ WDPT
2	θ WDPT	$K_{(-2\ \mathrm{cm})}$ S WDPT	θ WDPT	$K_{(-2\ \mathrm{cm})}$ S WDPT	θ WDPT	$K_{(-2\ \mathrm{cm})}$ S WDPT	θ WDPT	$K_{(-2\ \mathrm{cm})}$ S WDPT
3	$K_{(-2\ \mathrm{cm})}$ S WDPT	θ WDPT	$K_{(-2\ \mathrm{cm})}$ S WDPT	θ WDPT	$K_{(-2\ \mathrm{cm})}$ S WDPT	θ WDPT	$K_{(-2\ \mathrm{cm})}$ S WDPT	θ WDPT
4	θ WDPT	$K_{(-2\ \mathrm{cm})}$ S WDPT	θ WDPT	$K_{(-2\ \mathrm{cm})}$ S WDPT	θ WDPT	$K_{(-2\ \mathrm{cm})}$ S WDPT	θ WDPT	$K_{(-2\ \mathrm{cm})}$ S WDPT
5	$K_{(-2\ \mathrm{cm})}$ S WDPT	θ WDPT	$K_{(-2\ \mathrm{cm})}$ S WDPT	θ WDPT	$K_{(-2\ \mathrm{cm})}$ S WDPT	θ WDPT	$K_{(-2\ \mathrm{cm})}$ S WDPT	θ WDPT
6	θ WDPT	$K_{(-2\ \mathrm{cm})}$ S WDPT	θ WDPT	$K_{(-2\ \mathrm{cm})}$ S WDPT	θ WDPT	$K_{(-2\ \mathrm{cm})}$ S WDPT	θ WDPT	$K_{(-2\ \mathrm{cm})}$ S WDPT
7	$K_{(-2\ \mathrm{cm})}$ S WDPT	θ WDPT	$K_{(-2\ \mathrm{cm})}$ S WDPT	θ WDPT	$K_{(-2\ \mathrm{cm})}$ S WDPT	θ WDPT	$K_{(-2\ \mathrm{cm})}$ S WDPT	θ WDPT
8	θ WDPT	$K_{(-2\ \mathrm{cm})}$ S WDPT	θ WDPT	$K_{(-2\ \mathrm{cm})}$ S WDPT	θ WDPT	$K_{(-2\ \mathrm{cm})}$ S WDPT	θ WDPT	$K_{(-2\ \mathrm{cm})}$ S WDPT

Fig. 1. The spatial arrangement of hydraulic characteristics' measurements within the 8 x 8 square grid inside the 1-m^2 plot. The outer 10 cm wide frame area was left ungauged. $K_{(-2\ \mathrm{cm})}$ is the unsaturated hydraulic conductivity measured with minidisk infiltrometer, S is the sorptivity for water measured with minidisk infiltrometer, θ is the volumetric SWC and WDPT is the water drop penetration time test.

8 x 8 test squares at both depths. The outside 10-cm wide border around the measurement grid was left ungauged to ensure same lateral boundary conditions for all measurements (Fig.1).

The upper layer (5–10 cm depth) was removed immediately after the measurements finishing to minimize the influence on the underlying layer and measurements were repeated at the depth of 10 cm again. The parts, which were wetted by infiltrated water from the depth of 5 cm were avoided.

The water drop penetration time (WDPT) was measured to assess water repellency of soil surfaces. Three drops of distilled water from a medicinal dropper about volume of water 58 ± 5 µl were placed on a smoothed surface of a soil from the hight of about 20 mm. Time it took to penetrate the soil was recorded. Soil water repellency was measured on 64 squares at both, 5 cm and 10 cm depths, i.e. in all grid cells. Water repellency classes were distinguished as follows (Dekker and Ritsema, 1994): 1. wettable or non-water repellent (WDPT< 5 s); 2. slightly water repellent soil (WDPT = 5 – 60 s); 3. strongly water repellent soil (WDPT = 60 – 600 s); 4. severely water repellent soil (WDPT = 600 – 3600 s) and 5. extremely water repellent soil (WDPT > 3600 s).

Soil water content (SWC) was measured by Theta Probe Ml 2x (Delta T – Devices, Cambridge, England) at selected 32 grid cells as it is shown in Fig. 1. Sensor has four 6-cm long rods. Considering the measurement volume of this probe we assumed the data, measured when vertically installing sensor at the depth of 5 cm, represented soil water contents at both monitored soil depths (i.e. 5 cm and 10 cm). Since the soil at Mlaky II location is very rigid, coarse-textured, unstructured and with very low organic matter content, the Theta Probe was not specifically calibrated for this kind of soil, just the mode for mineral soils was selected during measurements.

Water infiltration was measured using Decagon minidisk infiltrometers (Decagon, 2007) with the disk radius of 2.25 cm at 32 positions at both depths in a such a way that squares with SWC measurements alternated with squares with infiltration measurements (Fig. 1). Small negative pressure head (h_0 = –2 cm) was applied at the infiltration interface.

Data measured using minidisk tension infiltrometers were used to calculate nearsaturated hydraulic conductivity. Two methods were applied. Zhang (1997) proposed to estimate the unsaturated hydraulic conductivity and sorptivity at suctions $h_0 \leq 0$ from the first two terms of the Philip´s infiltration equation (Philip, 1957):

$$I = a(h_0)\, t^{1/2} + b(h_0)\, t \qquad (1)$$

where I is the cumulative infiltration [L], h_0 is the applied suction [L], t is the time [T], $a(h_0)$ and $b(h_0)$ are the parameters of the second-order polynomial approximating the I-record versus $t^{1/2}$. The sorptivity and unsaturated hydraulic conductivity can then be calculated as:

$$S(h_0) = a(h_0) \qquad (2)$$

and

$$K(h_0) = \frac{b(h_0)}{A} \qquad (3)$$

where A is a constant and according to the Minidisc infiltrometer manual its value can either be selected for specific soil texture from the table (2.4 for sandy soil) or it can be calculated with using of soil water retention parameters (Decagon, 2007). To be consistent with previous researches (e.g. Orfánus et al., 2008, 2014) we used the recommended value 2.4.

For three-dimensional infiltration form the equation (1) has been modified as (Vandervaere et al., 1997):

$$I = St^{1/2} + (b + c)t \qquad (4)$$

where c is dependent on S, as follows:

$$c = \frac{\gamma S^2}{r_0(\theta_0 - \theta_n)} \qquad (5)$$

where γ is a proportionality constant and r_0 [L] is the radius of the disk (Haverkamp et al., 1994). θ_0 is the water content [% vol.] at applied potential head h_0 and θ_n is the initial water content of the soil [% vol.]. From this relationships it can be seen that S does not affect only the early stage of infiltration but via the c parameter also the steady stage of the process.

A variety of methods have been proposed to cope with this problem. Minasny and McBratney (2000) proposed For hydraulic conductivity ($K(h_0)$) at applied tension h_0 calculation based on Wooding´s (1968) analysis combined with macroscopic capillary length theory of White and Sully (1987):

$$K(h_0) = q_\infty - \frac{4xS^2}{(\theta_0 - \theta_n)\pi r_0} \qquad (6)$$

where q_∞ is the steady-state infiltration rate, x is a shape factor for the soil-water diffusivity function which is usually taken as 0.55 (White and Sully, 1987). S is the sorptivity estimated from Eq. (7) where they differentiated cumulative infiltration with respect to the square-root of time:

$$\frac{dI}{dt^{1/2}} = S + 2(b + c)t^{1/2} \qquad (7)$$

By plotting $dI/dt^{1/2}$ against $t^{1/2}$, and excluding the early time data which exhibit nonlinear behaviour, then fitting a line through the data with linear behaviour will give S as the intercept of the line.

The values of unsaturated hydraulic conductivity $K(h_0)$ (here $K_{(-2\ \mathrm{cm})}$) calculated by Eq. (3) and (6) , SWC and WDPT were processed statistically as for their distributions, basic statistics and mutual correlations. All statistical analyzes were performed at 0.05 significance level. The sorptivity parameter needed to calculate according to Eq. (6) was calculated from Eq. (7).

Since $K_{(-2\ \mathrm{cm})}$ and the SWC could not be measured at the same squares of the 8 x 8 measurement setup (Fig. 1) but were measured in rotation, their mutual correlation was investigated in a way that quadruplet of adjacent squares were merged into one larger square and couples of $K_{(-2\ \mathrm{cm})}$ values and SWC values inside such ensuing larger squares were averaged. The resulting measurement matrix providing 16 pairs of $K_{(-2\ \mathrm{cm})}$ vs. SWC values is outlined in Fig. 2.

To receive a demonstrative image of the spatial variability of these characteristics, the data were processed in Golden Software – Surfer7 into the form of contour maps. Radial basis function was used as a gridding method since the number of data was insuficient for kriging and among other methods provided by Surfer7 software it had produced the best cross-validation results. Radial basis functions are simple in implementation with sufficient smoothness and the Multiquadric basis

$({}^{1-1}K_{(-2\text{ cm})}+{}^{2-2}K_{(-2\text{ cm})})/2$ $({}^{1-1}S+{}^{2-2}S)/2$ $({}^{1-2}\theta+{}^{2-1}\theta)/2$	$({}^{3-1}K_{(-2\text{ cm})}+{}^{4-2}K_{(-2\text{ cm})})/2$ $({}^{3-1}S+{}^{4-2}S)/2$ $({}^{4-1}\theta+{}^{3-2}\theta)/2$	$({}^{5-1}K_{(-2\text{ cm})}+{}^{6-2}K_{(-2\text{ cm})})/2$ $({}^{5-1}S+{}^{6-2}S)/2$ $({}^{6-1}\theta+{}^{5-2}\theta)/2$	$({}^{7-1}K_{(-2\text{ cm})}+{}^{8-2}K_{(-2\text{ cm})})/2$ $({}^{7-1}S+{}^{8-2}S)/2$ $({}^{8-1}\theta+{}^{7-2}\theta)/2$
$({}^{1-3}K_{(-2\text{ cm})}+{}^{2-4}K_{(-2\text{ cm})})/2$ $({}^{1-3}S+{}^{2-4}S)/2$ $({}^{2-3}\theta+{}^{1-4}\theta)/2$	$({}^{3-3}K_{(-2\text{ cm})}+{}^{4-4}K_{(-2\text{ cm})})/2$ $({}^{3-3}S+{}^{4-4}S)/2$ $({}^{4-3}\theta+{}^{3-4}\theta)/2$	$({}^{5-3}K_{(-2\text{ cm})}+{}^{6-4}K_{(-2\text{ cm})})/2$ $({}^{5-3}S+{}^{6-4}S)/2$ $({}^{6-3}\theta+{}^{5-4}\theta)/2$	$({}^{7-3}K_{(-2\text{ cm})}+{}^{8-4}K_{(-2\text{ cm})})/2$ $({}^{7-3}S+{}^{8-4}S)/2$ $({}^{7-4}\theta+{}^{8-3}\theta)/2$
$({}^{1-5}K_{(-2\text{ cm})}+{}^{2-6}K_{(-2\text{ cm})})/2$ $({}^{1-5}S+{}^{2-6}S)/2$ $({}^{1-6}\theta+{}^{2-5}\theta)/2$	$({}^{3-5}K_{(-2\text{ cm})}+{}^{4-6}K_{(-2\text{ cm})})/2$ $({}^{3-5}S+{}^{4-6}S)/2$ $({}^{4-5}\theta+{}^{3-6}\theta)/2$	$({}^{5-5}K_{(-2\text{ cm})}+{}^{6-6}K_{(-2\text{ cm})})/2$ $({}^{5-5}S+{}^{6-6}S)/2$ $({}^{6-5}\theta+{}^{7-6}\theta)/2$	$({}^{7-5}K_{(-2\text{ cm})}+{}^{8-6}K_{(-2\text{ cm})})/2$ $({}^{7-5}S+{}^{8-6}S)/2$ $({}^{7-6}\theta+{}^{8-7}\theta)/2$
$({}^{1-7}K_{(-2\text{ cm})}+{}^{2-8}K_{(-2\text{ cm})})/2$ $({}^{1-7}S+{}^{2-8}S)/2$ $({}^{1-8}\theta+{}^{2-7}\theta)/2$	$({}^{3-7}K_{(-2\text{ cm})}+{}^{4-8}K_{(-2\text{ cm})})/2$ $({}^{3-7}S+{}^{4-8}S)/2$ $({}^{3-8}\theta+{}^{4-7}\theta)/2$	$({}^{5-7}K_{(-2\text{ cm})}+{}^{6-8}K_{(-2\text{ cm})})/2$ $({}^{5-7}S+{}^{6-8}S)/2$ $({}^{5-8}\theta+{}^{6-7}\theta)/2$	$({}^{7-7}K_{(-2\text{ cm})}+{}^{8-8}K_{(-2\text{ cm})})/2$ $({}^{7-7}S+{}^{8-8}S)/2$ $({}^{7-8}\theta+{}^{8-7}\theta)/2$

Fig. 2. Merging the original 64 squares within 0.64-m^2 plot into the 16 larger squares, each containing couple of $K_{(-2\text{ cm})}$, S and θ measurements. The upper indexes are the coordinates in measurement setup (see Figure 1).

function works quite well in most cases even with small number of data. To reduce the global influence of the transformation function we used the reciprocal Multiquadric method (Iske, 2003), which is recommended also by Carlson and Foley (1991).

RESULTS AND DISCUSSION

Measured wetting characteristics of soil and their spatial patterns

Measured values of WDPT at 5-cm depth are shown in Fig. 3a. The WDPT values ranged between 0 and 2640 s in depth of 5 cm and between 0 and 832 s in 10-cm depth. The distribution of WDPT classes at two depths is presented in Table 1.

Table 1. The distribution of WDPT classes at two depths over the 0.64 m^2 area of the research plot.

WDPT class/ Depth	Wettable	Slightly water repellent	Strongly water repellent	Severely water repellent	Extremely water repellent
5 cm	12	49	89	42	0
10 cm	51	118	19	4	0

The SWC (Fig. 3b) measured with the Theta probe ML 2X (Delta-T Devices) varied around the mean value of 10% vol. with the standard deviation (SD) = 2.5% vol. and variation coefficient 25% in the layer demarcated by these two soil depths, 5–10 cm. Field evidence for considerable SWC variation has been reported in water-repellent field soils (e.g. Hendrickx and Dekker (1991)).

The variation in SWC in presented study reaches the ceiling of the SWC variability ranges reported in classical works (Hills and Reynolds, 1969; Nielsen et al., 1973; Ritsema and Dekker, 1994; Warrick et al., 1977) but does not reach variations observed in water repellent soils (CV > 50% in Hendrickx and Dekker (1991) for instance). It can be a consequence of small spatial extent and relatively large measurement scale (75 cm^3) of the theta probe, which smooths the variability in SWC at smaller scales.

The spatial distribution of $K_{(-2\text{ cm})}$ values calculated according to Zhang (1997) - Eq. (3) are shown in Fig. 3c for the 5-cm depth and in Fig. 3d for 10-cm depth.

The $K_{(-2\text{ cm})}$ mean value (calculated for a lognormal distribution) at the 5-cm depth was 0.001 cm s^{-1} with standard deviation (SD) = 0.0008 cm s^{-1} while at 10 cm depth the mean value was 0.0014 cm s^{-1} with SD = 0.002 cm s^{-1}. The frequency histograms of $K_{(-2\text{ cm})}$ for two soil layers are in Fig. 4 and unlike their variances, the mean values do not differ significantly at 0.05 significance level (Fig. 5). Approximation of the cumulative infiltration vs. square root of time record by polynom provided unrealistic values of $K_{(-2\text{ cm})}$ in 5 cases at depth of 5 cm. These values were not considered in further processing.

The $K_{(-2\text{ cm})}$ mean value calculated according to Minasny and McBratney (2000) - Eq. (6) at 10 cm depth was 0.00293 cm s^{-1} with SD = 0.0022 cm s^{-1}. The data and the frequency histograms of $K_{(-2\text{ cm})}$ calculated for the 10-cm horizon by two different methods (Eq. 3 and Eq. 6) are in (Table 2) and Fig. 5.

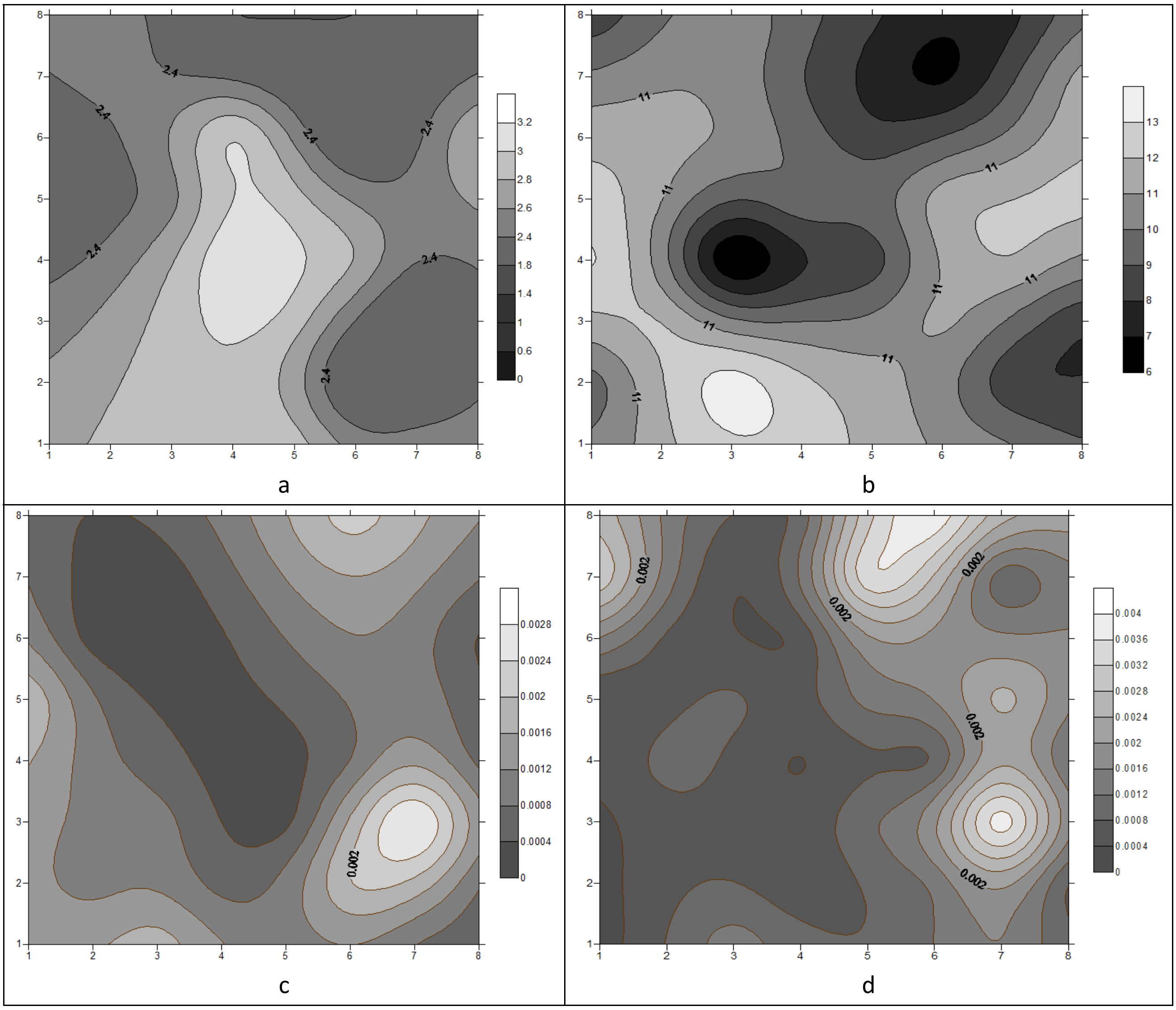

Fig. 3. The contour maps of log(WDPT in s) at 5-cm depth (a), soil water content in volumetric % (b), unsaturated hydraulic conductivity, $K_{(-2\ \mathrm{cm})}$ in cm s^{-1} at 5-cm (c) and 10-cm (d) depths calculated according to Zhang (1997).

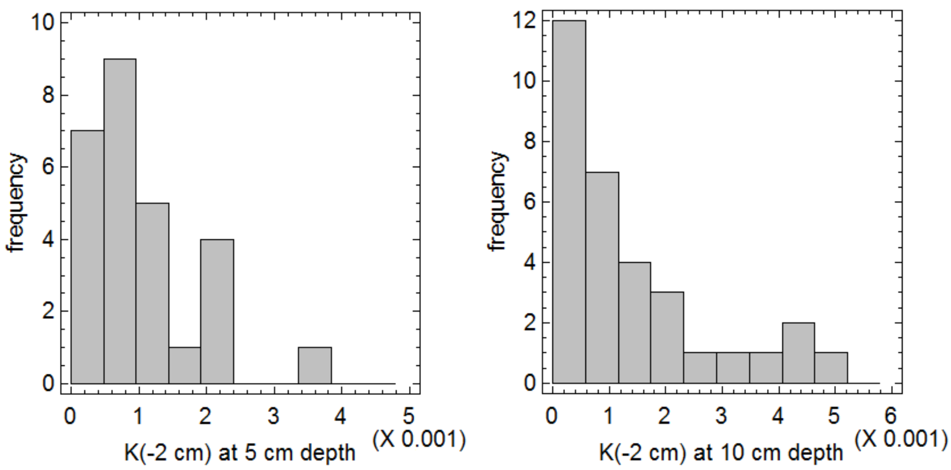

Fig. 4. Frequency histograms of unsaturated hydraulic conductivity, $K_{(-2\ \mathrm{cm})}$ (in cm s^{-1}) at 5-cm depth (27 measurements - left) and at 10-cm depth (32 measurements - right) calculated according to Zhang (1997).

Table 2. Comparison of $K_{(-2\ cm)}$ values (in cm s^{-1}) calculated by two methods; Zhang (1997) and Minasny and McBratney (2000).

$K_{(-2\ cm)}$ – Minasny and McBratney	$K_{(-2\ cm)}$ - Zhang	$K_{(-2\ cm)}$ – Minasny and McBratney	$K_{(-2\ cm)}$ - Zhang
1.22E-04	1.25E-04	1.79E-03	5.00E-04
4.08E-04	2.50E-04	1.68E-03	1.75E-03
3.64E-04	2.08E-04	5.32E-03	4.38E-03
6.76E-03	3.63E-03	4.41E-03	3.00E-03
1.70E-03	6.67E-04	2.95E-03	1.75E-03
3.21E-03	1.13E-03	5.83E-03	2.33E-03
1.53E-03	5.42E-04	2.14E-03	7.92E-04
3.30E-03	1.38E-03	2.50E-03	1.33E-03
2.33E-03	1.63E-03	3.53E-03	1.54E-03
1.23E-03	6.25E-04	8.70E-03	5.00E-03
1.96E-03	1.08E-03	2.43E-03	7.92E-04
8.05E-04	2.92E-04	1.13E-03	6.05E-04
8.84E-04	3.33E-04	2.06E-03	1.09E-03
7.86E-04	1.67E-04	8.35E-04	2.98E-04
8.23E-03	4.25E-03	7.84E-04	4.33E-04
4.63E-04	1.25E-04	7.86E-04	1.17E-04

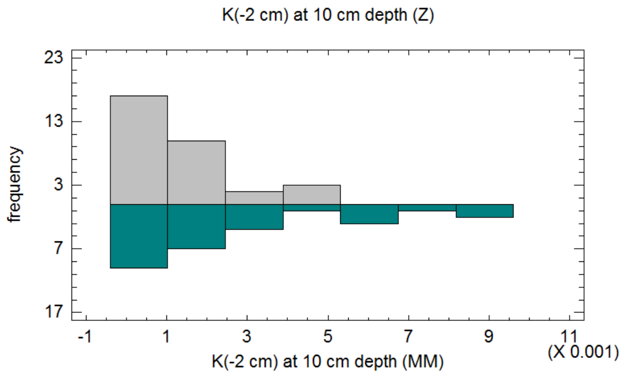

Fig. 5. Frequency histograms of unsaturated hydraulic conductivity, $K_{(-2\ cm)}$ (in cm s^{-1}) values at 10-cm soil depth calculated according to Zhang's Eqs. 2–3 (up - Z) and according to Minasny and McBratney (low - MM).

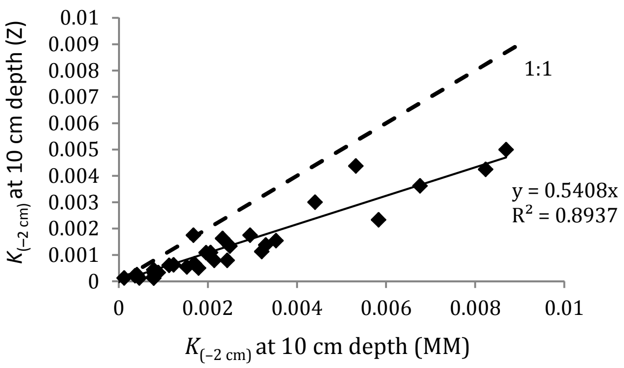

Fig. 6. Regression analyses between values of unsaturated hydraulic conductivity, $K_{(-2\ cm)}$ (in cm s^{-1}) at 10-cm soil depth, calculated according to Zhang's Eq. 3 (Z) and according to Minasny and McBratney Eq. 6 (MM). The dashed is the 1:1 line.

In Fig. 6, there is a regression analyses between the $K_{(-2\ cm)}$ values calculated according to Eq. (3) and according to Eq. (6), respectively. The values calculated according to Zhang (1997) are underestimated roughly by half against the values calculated according to Minasny and McBratney (2000).

Mutual relationships between measured wetting characteristics

The values of $K_{(-2\ cm)}$ at two particular depths were intercorrelated with medium level of statistical dependence (Fig. 7 and Table 3) what indicates that the change in wetting characteristics of soil with depth is rather gradual then abrupt and that the upper more water repellent layer may perform as distribution layer for the lower less water repellent one (Hendrickx and Yao, 1996).

The $K_{(-2\ cm)}$ values at depth of 5 cm showed to be indirectly proportional to SWC and WDPT as well, with strong level of dependency (Table 3) in latter case. About one half of the $K_{(-2\ cm)}$ variability was explained by persistency of soil water repellency quantified by WDPT (R^2 = 0.49). This supports the observations of Orfánus et al. (2014) for pairs of $K_{(-2\ cm)}$ vs. WDPT collected across several dry spells (during years 2005–2010) at the same location. This dependency decreases at 10-cm depth to the weak level what is related to overall decrease in water repellency persistency as well as its areal variability (mean WDPT at 5 cm is 482.90 s with SD = 665.315 s while mean WDPT at 10 cm is 50.42 s with SD = 115.45 s) with depth. Similarly, the WDPT showed to be indirectly proportional to SWC with medium dependency level (Table 3). It can be stated that in sandy soil under the grass cover (with species' composition as described in the methods section of this paper) at scale of 0.64 m^2 there was detected soil water repellency in a range from perfectly wettable (locally and only at 10-cm depth) to severally water repellent soil. The level of water repellency and its variability seems to be determined not only by vegetation structure and products of their decomposition but the variability of SWC as well. Notwithstanding, the option that this relationship works in opposite direction (soil water repellency determines the wetting pattern) comes to consideration as well (Hendrickx and Flury, 2001).

It is obvious that in our studied soil material the water repellency determines to a certain extent values of $K_{(-2\ cm)}$ calculated according to Eq. (3) and their spatial distribution. The strength of this relationship decreases with soil depth and humidity of weather seasons (in Table 3 and also in Orfánus et al., 2014).

Table 3. Correlation coefficients between the evaluated parameters (n = 27, * significant at α = 0.05, ** significant at α = 0.01). $K_{(-2\ cm)}$ is the unsaturated hydraulic conductivity (in cm s^{-1}) measured with minidisk infiltrometer and calculated according to Zhang (1997) – a or Minasny and McBratney (2000) – b, θ is the SWC (volumetric %) and WDPT is the water drop penetration time (s).

	$K_{(-2\ cm)}$ at 10-cm depth	log(WDPT) at 5 or 10-cm depth	θ
$K_{(-2\ cm)}$ at 5-cm depth	0.48**	–0.70**	–0.16
$K_{(-2\ cm)}$ at 10-cm depth - a		–0.37	–0.45*
$K_{(-2\ cm)}$ at 10-cm depth - b		–0.24	–0.24
log(WDPT) at 5-cm depth			–0.41*
log(WDPT) at 10-cm depth			–0.21

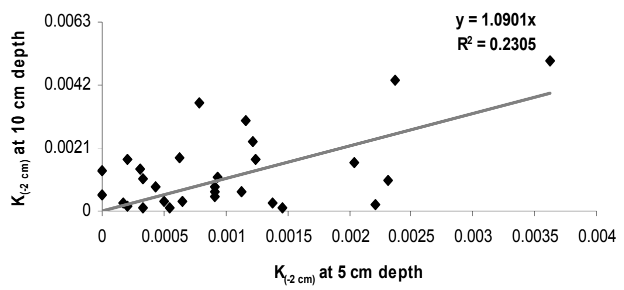

Fig. 7. Linear interdependence between the unsaturated hydraulic conductivities, $K_{(-2\ cm)}$ (in cm s^{-1}) calculated according to Zhang (1997) at 5- and 10-cm depths.

The pseudocorrelation between SWC and $K_{(-2\ cm)}$

The indirect proportionality of $K_{(-2\ cm)}$ calculated by Eq. (3) with antecedent SWC with medium level of dependency (r = –0.49) was detected at the depth of 10 cm (Table 3). Actually there is no rationale behind such relationship since $K_{(-2\ cm)}$ relates to steady state phase of infiltration, when it is expected that conductive zones under the infiltrometer disk have already reached the maximal water content and it is no more changing. This relationship was not detected in depth of 5cm in our study, however Jirků et al. (2013) observed similar relationship between $K_{(-2\ cm)}$ and field SWC in Greyic Phaeozem while no statistically significant dependence was confirmed in Haplic Luvisol and Haplic Cambisol (Jirků et al., 2013).

Vandervaere et al. (1997) state correctly that the influence of sorptivity and initial unsaturation of soil when approximating the infiltration record by polynom in sense of Zhang (1997) is high even at the steady-stage of the infiltration process. Such effect is most probably the primary cause for the detected proportionality between $K_{(-2\ cm)}$ calculated by Eq. (3) and SWC at 10-cm depth. After we recalculated the $K_{(-2\ cm)}$ values according to Eq. (6) using S (sorptivity) parameter estimated by Eq. (7) in sense of Minasny and McBratney (2000), this pseudo-dependency of $K_{(-2\ cm)}$ on SWC decreased to insignificant level (r = –0.24). In the upper soil layer at 5-cm depth, this artificial dependency between $K_{(-2\ cm)}$ and antecedent SWC was not observed. It is most probable that the effect of initial unsaturation of soil and sorptivity in this material was substantially inhibited by strong water repellency (Orfánus et al., 2014).

On the other hand, as the result of edge effect Kodešová et al. (2011) observed overestimation of $K_{(-2\ cm)}$ calculated by Zhang (1997) when compared to $K_{(-2\ cm)}$ calculated according to Wooding (1968) when small-disk infiltrometer was used.

CONCLUSIONS

1. The studied grassland sandy soil in SW Slovakia with semiarid climate is susceptible to water repellency emergence. The persistency of soil water repellency can vary across 4 SWR classes from wettable to severely water repellent at scale of 0.64 m^2 within soil subsurface horizons of 5 and 10 cm depths. The level of SWR and its variability are significantly interrelated with the variability of SWC and variability of unsaturated hydraulic conductivity. The spatial variability of soil water repellency determines the resulting wetting patterns in this soil, which exhibited certain level of spatial continuity between depths of 5–10 cm. It was manifested in this study by significant mutual correlation between $K_{(-2\ cm)}$ estimated at both depths. To relate this continuity with what is called fingered flow in the literature deserves more concern and investigation in the future.
2. The values of $K_{(-2\ cm)}$ calculated from minidisk infiltrometers according to classical method proposed by Zhang (1997) may be significantly underestimated and artificially pseudocorrelated with antecedent SWC in a way that the site with lower antecedent water content has higher $K_{(-2\ cm)}$ value. This misleading pseudocorrelation caused by the effect of initial unsaturation of soil (via sorptivity parameter) can be corrected by calculating sorptivity and $K_{(-2\ cm)}$ according to approaches published in Minasny and McBratney (2000). Since sorptivity was mostly close to zero in the strongly water repellent soil at depth of 5 cm, it has not influenced the steady stage of infiltration and calculation of $K_{(-2\ cm)}$ according to Zhang (1997) did not result in pseudocorrelation with antecedent SWC.

Acknowledgement. This study was supported by national grant agency VEGA –project No. 2/0152/15, Slovak-Hungarian bilateral project MAD SNK-5/2013 and partially also by the Research and Development Operational Programme, the project Excellence Centre of Integral Territory Flood Protection, code ITMS 26240120004, funded by the European Regional Development Fund (ERDF).

REFERENCES

Bedrna, Z., Orfánus, T., 2013. A new classification of soil textures and its application to the geography of soils in Slovakia. Geografický Časopis, 65, 2, 161–169. (In Slovak.)

Carlson, R.E., Foley, T.A., 1991. Radial Basis Interpolation Methods on Track Data. Lawrence Livermore National Laboratory, Livermore, CA, USA. UCRL-JC-1074238

Close, K.R., Frasier, G., Dunn, G.H., Loftis, J.C., 1998. Tension infiltrometer contact interface evaluation by the use of potassium iodide tracer. Trans. ASAE, 41, 995–1004.

Decagon, 2007. Minidisk Infiltrometer User's Manual. Version 6. Decagon Devices, Inc., Pullman.

Dekker, L.W., Ritsema, C.J., 1994. How water moves in a water-repellent sandy soil: 1. Potential and actual water repellency. Water Resources Research, 30, 2507–2517.

Dekker, L.W., Ritsema, C.J., Wendroth, O., Jarvis, N., Oostindie, K., Pohl, W., Larsson, M., Gaudet, J., 1999.

Moisture distribution and wetting rates of soils at experi-experimental fields in the Netherland, France, Sweden and Germany. Journal of Hydrology, 215, 4–22.

Dekker, L.W., Doerr, S.H., Oostindie, K., Ziogas, A.K., Ritsema, C.J., 2001. Water repellency and critical soil water content in a dune sand. Soil Science Society of America Journal, 65, 6, 1667–1674.

Doerr, S.H., Thomas, A.D., 2000. The role of soil moisture in controlling water repellency: new evidence from forest soils in Portugal. Journal of Hydrology, 231–232, 134–147.

Doerr, S.H., Shakesby, R.A., Walsh, R.P.D., 2000. Soil water repellency: its causes, characteristics and hydro-geomorphological significance. Earth-Science Reviews, 51, 33–65.

Dohnal, M., Dusek, J., Vogel, T., 2010. Improving hydraulic conductivity estimates from minidisk infiltrometer measurements from soils with wide pore-size distributions. Soil Science Society of America Journal, 74, 804–811.

Fodor, N., Sándor, R., Orfanus, T., Lichner, L., Rajkai, K., 2011. Evaluation method dependency of measured saturated hydraulic conductivity. Geoderma, 165, 60–68.

Goebel, M.O., Bachmann, J., Reichstein, M., Janssens, I.A., Guggenberger, G., 2011. Soil water repellency and its implications for organic matter decomposition – is there a link to extreme climatic events? Global Change Biology, 17, 2640–2656.

Green, T.R., Ahuja, L.R., Benjamin, J.G., 2003. Advances and challenges in predicting agricultural management effects on soil hydraulic properties. Geoderma, 116, 3–27.

Hallett, P.D., Nunan, N., Douglas, J.T., Young, I.M., 2004. Millimeter-scale spatial variability in soil water sorptivity: scale, surface elevation, and subcritical repellency effects. Soil Science Society of America Journal, 68, 352–358.

Haverkamp, R., Ross, P.J., Smettem, K.R.J., Parlange, J.Y., 1994. Three-dimensional analysis of infiltration from the disk infiltrometer. 2. Physically based infiltration equation. Water Resources Research, 30, 2931–2935.

Hendrickx, J.M.H., Dekker, L.W., 1991. Experimental evidence of unstable wetting fronts in non-layered soils. In: Gish, T.J., Shirmohammadi, A. (Eds): Proc. ASAE National Symposium on Preferential flow, Chicago, Illinois, pp. 22–31.

Hendrickx, J.M.H., Yao, T.M., 1996. Prediction of wetting front stability in dry field soils using soil and precipitation data. Geoderma, 70, 2–4, 265–280.

Hendrickx, J.M.H., Flury, M., 2001. Uniform and preferential flow mechanisms in the vadose zone. In: National Research Council (Eds.): Conceptual Models of Flow and Transport in the Fractured Vadose Zone. National Academy Press, Washington DC, pp. 149–187.

Hills, R.C., Reynolds, S.G., 1969. Illustrations of soil moisture variability in selected areas and plots of different sizes. Journal of Hydrology, 8, 27–47.

Iske, A., 2003. Radial basis functions: basics, advanced topics and meshfree methods for transport problem. Seminar of Mathematics, pp. 247–274.

Jirků, V., Kodešová, R., Nikodem, A., Mühlhanselová, M., Žigová, A., 2013. Temporal variability of structure and hydraulic properties of topsoil of three soil types. Geoderma, 204–205, 43–58.

Kodešová, R., Jirků, V., Kodeš, V., Mühlhanselová, M., Nikodem, A., Žigová, A., 2011. Soil structure and soil hydraulic properties of Haplic Luvisol used as arable land and grassland. Soil & Tillage Research, 111, 154–161.

Kořenková, L., Šimkovic, I., Dlapa, P., Juráni, B., Matúš, P., 2015. Identifying the origin of soil water repellency at regional level using multiple soil characteristics: The White Carpathians and Myjavska pahorkatina Upland case study. Soil & Water Research, 10, 2, 78–89.

Leighton-Boyce, G., Doerr, S.H., Shakesby, R.A, Walsh, R.P.D., Ferreira, A.J.D., Boulet, A.K., Coelho, C.O.A., 2005. Temporal dynamics of water repellency and soil moisture in eucalypt plantations, Portugal. Australian Journal of Soil Research, 43, 3, 269–280.

Letey, J., Carrillo, M.L.K., Pang, X.P., 2000. Approaches to characterize the degree of water repellency. Journal of Hydrology, 231–232, 61–65.

Lichner, Ľ., Babejová, N., Dekker, L.W., 2003. Effects of kaolinite and drying temperature on the persistence of soil water repellency induced by humic acids. Rostlinná Výroba, 48, 203–207.

Lichner, L., Eldridge, D.J., Schacht, K., Zhukova, N., Holko, L., Šír, M., Pecho, J., 2011. Grass cover influences hydrophysical parameters and heterogeneity of water flow in a sandy soil. Pedosphere, 21, 6, 719–729.

Mataix-Solera, J., Arcenegui, V., Guerrero, C., Jordán, M., Dlapa, P., Tessler, N.,Wittenberg, L., 2008. Can terra rossa become water repellent by burning? A laboratory approach. Geoderma, 147, 178–184.

Minasny, B., McBratney, A.B., 2000. Estimation of sorptivity from disk-permeameter measurements. Geoderma, 95, 305–324.

Nielsen, D.R., Biggar, J.W., Erh, K.T., 1973. Spatial variability of field - measured soil – water properties. Hilgardia, 42, 215–259.

Orfánus, T., Bedrna, Z., Lichner, Ľ., Hallett, P.D., Kňava, K., Sebíň, M., 2008. Spatial variability of water repellency in pine forest soil. Soil & Water Research, 3, Special Issue 1, 123–129.

Orfánus, T., Dlapa, P., Fodor, N., Rajkai, K., Sándor, R., Nováková, K., 2014. How severe and subcritical water repellency determines the seasonal infiltration in natural and cultivated sandy soils. Soil & Tillage Research, 135, 49–59.

Pekárová, P., Pekár, J., Lichner, Ľ., 2015. A new method for estimating soil water repellency index. Biologia, 70, 11, 1450–1455.

Philip, J.R., 1957. The theory of infiltration: 4. Sorptivity and algebraic infiltration equations. Soil Science, 84, 257–264.

Ritsema, C.J., Dekker, L.W., 1994. Soil moisture and dry bulk density patterns in bare dune sands. Journal of Hydrology, 154, 107–131.

Ritsema, C.J., Dekker, L.W., van der Elsen, E.G.M., Oostindie, K., Nieber, J.L., 1997. Recurring fingered flow pathways in a water repellent sandy field soil. Hydrology and Earth System Sciences, 4, 777–786.

Ritsema, C.J., van Dam, J.C., Dekker, L.W., Oostindie, K., 2005. A new modelling approach to simulate preferential flow and transport in water repellent porous media: Model structure and validation. Australian Journal of Soil Research, 43, 361–369.

Schlesinger, W.H., Raikes, J.A., Hartley, A.E., Cross, A.F., 1996. On the spatial pattern of soil nutrients in desert ecosystem. Ecology, 77, 364–374.

Taiz, L., Zeiger, E., Møller, I.M., Murphy, A., 2015. Plant Physiology and Development. 6th Edition. Sinauer Associates, Inc, Sunderland, Massachusetts, USA, 761 p. ISBN: 978-1-60535-255-8

Täumer, K., Stoffregen, H., Wessolek, G., 2005. Determination of repellency distribution using soil organic matter and water content. Geoderma, 125, 1–2, 107–115.

Tillman, R.W., Scotter, D.R., Wallis, M.G., Clothier, B.E., 1989. Water repellency and its measurement by using intrinsic sorptivity. Australian Journal of Soil Research, 27, 637–644.

Vandervaere, J.P., Peugeot, C., Vauclin, M., Angulo Jaramillo, R., Lebel, T., 1997. Estimating hydraulic conductivity of crusted soils using disk infiltrometers and minitensiometers. Journal of Hydrology, 188–189, 209–223.

Warrick, A.W., Mullen, G.J., Nielsen, D.R., 1977. Predictions of the soil water flux based upon field-measured soil-water properties. Soil Science Society of America Journal, 41, 14–19.

White, I., Sully, M.J., 1987. Macroscopic and microscopic capillary length and time scales from field infiltration. Water Resources Research, 23, 1514–1522.

Wooding, R., 1968. Steady infiltration from a shallow circular pond. Water Resources Research, 4, 1259–1273.

WRB, 2014. E-ISBN 978-92-5-108370-3 (PDF).

Zhang, R., 1997. Determination of soil sorptivity and hydraulic conductivity from the disk infiltrometer. Soil Science Society of America Journal, 61, 1024–1030.

Received 30 April 2015
Accepted 24 November 2015